

Power Normalization Perspective for massive MIMO Network using MMSE Precoding Techniques

^{1*} Eze, Gerald C., ²Ahaneku, Mamilus A., and ³Chijindu, Vincent C.

¹Department of Electronic/Electrical Engineering, Federal Polytechnic, Oko, Aguata, Anambra State, Nigeria.

^{2,3}Department of Electronic Engineering, University of Nigeria, Nsukka, Enugu State, Nigeria.

DOI : <https://doi.org/10.51583/IJLTEMAS.2024.130518>

Received: 01 May 2024; Revised: 12 May 2024; Accepted: 17 May 2024; Published: 15 June 2024

Abstract: This paper seeks ways to improve spectral efficiency (or throughput) while mitigating multi-user interferences for large-scale antenna arrays, massive multiple input multiple output (mMIMO) systems via the use of the minimum mean squared error (MMSE) precoding schemes. The impact of the power at the user equipment (UEs) being adjusted to meet the transmission power constraint of the BS otherwise known as power normalization on the performance of the single and multi-cell MMSE precoders (S-MMSE and M-MMSE) was studied. The choice of power normalization (matrix normalization or vector normalization) and how they can impact worse or better performances on S-MMSE and M-MMSE under three different channel estimates with respect to varying pilot reuse factors were simulated and analyzed. We considered a downlink mMIMO network model that accounts for the number of antennas and single-antenna UEs. Numerical results obtained after simulations depict that M-MMSE with vector normalization (VN) out-performs S-MMSE with vector/matrix normalization and M-MMSE with matrix normalization (MN) by having the highest average sum SE, throughput, and signal-to-interference plus noise ratio (SINR/SNR) for any number of antennas and UEs in the three-channel estimators. LS channel estimator performs the least when compared to EW-MMSE and MMSE channel estimators.

Keywords: power normalization, matrix normalization, vector normalization, S-MMSE, M-MMSE

I. Introduction

The massive multi-input multi-output (m MIMO) network is an extended MIMO wireless communication technology that serves several mobile users or users equipment (UEs) simultaneously in the same frequency-time resource [1]. MIMO networks are an integral component of present wireless networks, and in recent years they have been used widely to achieve high spectral efficiency (SE) and data throughput. Before the inception of MIMO, single-input-single-output (SISO) network were mostly used, which had very low SE and throughput and could not serve a large number of UEs with high reliability. To accommodate this huge demand for data traffic, various new MIMO technology like single-user MIMO (SU-MIMO), multi-user MIMO (MU-MIMO), and distributed MIMO were introduced and developed. However, these new technologies are also not enough to accommodate the ever-increasing data traffic. The wireless UEs have increased drastically in the last few years, and these UEs produce trillions of data that must be handled efficiently with more reliability. The current MIMO technologies associated with 4G/LTE network is unable to handle this large influx in data traffic with more speed and reliability. Therefore, the 5G and next-generation networks have considered m MIMO technology as a key enabling technology needed to overcome the challenges created by large-scale data traffic and UEs [1, 15].

In m MIMO, precoding is a signal processing technique that is required to direct transmitted signals towards the UEs. Precoding is usually performed at the base station (BS) before signal transmission in order to mitigate the impact of pilot contamination [2-3]. Linear precoding has a critical role in m MIMO

and the basic linear precoding schemes are the maximum ratio (MR), zero-forcing (ZF), regularized zero-forcing (RZF), single-cell minimum mean squared error (S-MMSE), and multi-cell minimum mean squared error (M-MMSE). The main objective of precoding in m MIMO systems is to improve the gain of the large-scale antenna array and mitigate the impact of multiuser interference [4]. In order to utilize basic linear precoding, it is required that the power at the UEs be adjusted to meet the transmission power constraint of the BS and this is known as precoding power normalization [5, 11]. Power normalization is categorized into two major techniques: vector normalization (VN) and matrix normalization (MN) [5-12]. MN assigns different powers to UEs and applies the same precoding weight to UEs by normalizing over all UEs ($\mathbb{E} \left\{ \frac{\mathbf{F}}{\|\mathbf{F}\|_F} \right\}$). In contrast, VN assigns same power to UEs and generates different precoding weight for each UE separately ($\mathbb{E} \left\{ \frac{\mathbf{f}}{\|\mathbf{f}\|} \right\}$), which results in different throughput among UEs [12].

The selection of the precoding weight, \mathbf{F} in MN will determine how the transmit power is allocated between the different UEs. Hence, power allocation is determined by the precoders. For instance, MR allocates less power to UEs with weak channels than UEs with strong channels, while ZF does the opposite. Hence, if one tries to compare MR and ZF under MN, the different power

allocations will have strong leverage on the results [5-12]. The aforementioned problem was resolved with VN and VN method is employed more often in the literature than MN. With VN, power allocation is not determined by the precoders. However, the main problem with VN is the same power P is allocated to the UEs, K ($\mathbb{E} \left\{ \sqrt{\frac{P}{K}} \right\}$), which is undesirable if some UEs have weak channels and others have strong channels. A conscious decision therefore should be made when it comes to power normalization and precoders between UEs. In this paper, we consider the MMSE precoders with power normalization.

A. Related works

The performance analysis of linear precoding techniques for downlink transmissions in single-cell m MIMO Systems was done in [6 - 8] using power normalization. The tested linear precoding techniques considered in [6] were ZF, MR, RZF and the truncated polynomial expansion (TPE), while MR and ZF were considered in [7] and [8]. The results analyzed show that power normalization for MR gives good performance at low downlink transmission power while ZF produces good performance at high downlink transmission power. Studies on how vector normalization (VN) and matrix normalization (MN) techniques affect the performance of MR, ZF, and RZF precoding in multi-cell m MIMO were presented in [5] and [9-11], respectively. The results show that VN largely outperforms MN for MR, ZF, and RZF. An analysis done in [9] and [10] aims to determine the performance of m MIMO for cell-boundary users. Presented results show that for the downlink, VN is better for ZF while MN is better for MR at low signal-to-noise-ratio (SNR) regardless of number of cell-boundary UEs. In contrast, for the uplink, MR should be used instead of ZF at low SNR. In [5], the authors showed that MN and VN treat the noise and interference in the same manner, but have different effects on pilot contamination and received signal power. This implies that in massive MIMO, non-coherent interference and noise, rather than pilot contamination, are often the major limiting factors of considered precoding schemes. In [11], a validated asymptotic analysis for different values of the number of antennas (M) and UEs (K) was investigated. The results showed that the number of antennas required to achieve a target sum rate with VN is smaller than the one required by MN by a factor of 3 or 4. In [12], the authors researched on the impact of the power normalization in MU-MIMO. Quality indexes such as system capacity and fairness were presented while considering user scheduling. Simulation results show that VN limits the fairness index (FI), while performing better than MN in system capacity. However, although the MN falls behind VN in terms of the system capacity, MN has superiority in fairness. Therefore, VN is effective in the relatively low FI. MN is appropriate for improving the FI while losing a certain amount of system capacity.

The above related works considered power normalization on single-cell precoding schemes such as MR, ZF, and RZF in the m MIMO networks. The effect of power normalization on multi-cell precoding scheme has not been thoroughly investigated yet. However, a detailed treatment of the impact of power normalization on multi-cell precoder does not exist in the literature. The aim of this paper is to fulfill this research gap by investigating the effect of power normalization on MMSE precoding schemes such as S-MMSE and M-MMSE with reference to the pilot reuse factor, correlation channels, SNR/SINR as well as the number of antennas and UEs in massive MIMO Networks. The MMSE precoding schemes have an acceptable performance required to mitigate intra-cell and multi-cell interference [13-14, 20]. The main contributions of this work are:

- To elaborate and analyze power normalization techniques using MMSE precoding schemes.
- To show how the choice of power normalization affects the performance of S-MMSE and M-MMSE under different channel estimates with respect to the pilot reuse factor.

II. System Model and Power Normalization Techniques

We consider the downlink of a m MIMO cellular network with multi-cell network of up to 16 cells. The BS of each cell has M antennas and serves K single-antenna UEs in the same time-frequency resource. The system model for downlink (DL) may be determined as given in [15]:

$$y_{jk} = \sum_{j=1}^L (h_{jk}^j)^H s_j + n_{jk} \quad (1)$$

L indicates the number of cells, $(\cdot)^H$ indicates the Hermitian transpose matrix operator and the received DL signal $y_{jk} \in \mathbb{C}^{M \times K}$ at UE k in cell j is modeled above. $h_{jk}^j \in \mathbb{C}^{M \times K}$ is them MIMO DL channel matrix, where \mathbb{C} denotes a complex value matrix, M is the number of BS antennas and it represents the number of rows in the matrix. K is the number of UEs which represents the number of columns in the matrix, j superscript denotes the BS's cell index and jk subscripts denote k th UE in cell j .

$$h_{jk}^j = N_C(0, R_{jk}^j) \quad (2)$$

h_{jk}^j is the correlated Rayleigh channel and $R_{jk}^j \in \mathbb{C}^{M \times M}$ is the spatial correlation matrix, where j superscript represents the BS's cell index and jk subscripts represent k th UE in cell j . h_{jk}^j is modeled by circularly symmetric complex Gaussian distribution having circular symmetry N_C with zero mean and the spatial correlation matrix. The receiver noise may be expressed as

$$n_{jk} = N_C(0, \sigma^2) \quad (3)$$

Where $n_{j,k}$ represents the additive white Gaussian noise (AWGN) vector and s_j is the DL transmit signal [15-16].

A. Downlink Channel Estimators

For efficient usage of BS antennas, each BS is required to acquire knowledge of the channels from the UEs which are active in the coherence block [17]. The BS j estimates the channels knowledge from its UEs in a particular cell j . The massive MIMO network being considered operates according to the time division duplex (TDD) protocol. The TDD protocol which was discussed extensively in [13, 14] allows the downlink channel estimates to be determined from the uplink pilot signal by exploiting channel reciprocity. The uplink pilot signal Y_j^P received at BS j defined in [15, 17] is expressed in equation (4).

$$Y_j^P = \sum_{k=1}^{k_j} \sqrt{p_{jk}} h_{jk}^j \vartheta_{jk}^T + \sum_{\substack{l=1 \\ l \neq j}}^L \sum_{i=1}^{k_l} \sqrt{p_{li}} h_{li}^j \vartheta_{li}^T + N_j^P \quad (4)$$

The first part in Equation (4) denotes the desired pilots in the cell, the second part denotes the interfering pilots from other adjacent cells and then the third part N_j^P denotes the receiver noise.

Matrix $N_j^P \in \mathbb{C}^{M \times \tau_p}$ contains independent identically distributed elements which follow a complex Gaussian distribution with zero mean and noise variance σ^2 . p_{jk} is the deterministic uplink pilot signal and power coefficient for the pilot of user k in cell j . In the channel estimation phase, the aggregated received uplink pilot signals at BS j are denoted as $Y_j^P \in \mathbb{C}^{M \times \tau_p}$ where τ_p is the length of a pilot sequence (and also equals to the number of orthogonal pilot sequences available for the network). Generalized pilot reuse was supported by denoting the relation between τ_p and K using the expression $\tau_p = fK$, where f is the pilot reuse factor (1, 2, 4 or 16) [17]. The universal pilot reuse factor is $f=1$ while the non-universal pilot reuse factors are $f=2, 4, 16$ [11]. The mutually orthogonal uplink pilot matrix τ_p was organized as columns at BS j , $\vartheta_j = [\vartheta_{j1}, \vartheta_{j2}, \vartheta_{j3}, \dots, \vartheta_{jk}] \in \mathbb{C}^{\tau_p \times K}$ which were transmitted by the k th UE of the cell j . All pilot sequences are assumed to originate from a predefined orthogonal pilot book in which sequence $\vartheta_{li}^T \in \mathbb{C}^{\tau_p}$ was defined [15, 17] and expressed in equations (5a) to equation (6):

BS j correlates Y_j^P with ϑ_{jk}^* to estimate y_{jk}^j .

$$y_{jk}^j = Y_j^P \vartheta_{jk}^* \quad (5a)$$

$$\vartheta_{jk}^H \vartheta_{ik} = \begin{cases} \tau_p & \text{when } j = i \\ 0 & \text{when } j \neq i \end{cases} \quad (5b)$$

i. MMSE Channel Estimator may be expressed in equation (6) as obtained in [15] and [17]

$$\hat{h}_{jk}^j = \sqrt{p_{jk}} R_{jk}^j Z_{jk}^j y_{jk}^j \quad (6)$$

$$Z_{jk}^j = \left(\sum_{(j',k') \in q} p_{j'k'} \tau_p R_{j'k'}^j + \sigma^2 I_M \right)^{-1} \quad (7a)$$

$R_{jk}^j \in \mathbb{C}^{M \times M}$ is the spatial correlation matrix, where j superscript represents the BS's cell index and jk subscripts represent k th UE in cell j . Z_{jk}^j is the matrix of the inverse of the normalized processed signal correlation matrix defined in [15].

$$q = \{(j', k') : \vartheta_{jk} = \vartheta_{j'k'}, j' = 1, 2, 3 \dots j, k' = 1, 2, 3 \dots k\} \quad (7b)$$

τ_p samples are reserved for UL pilot signaling in each coherence block. The set above defines the indices of all mobile terminals (UEs) that use the same pilot sequence as user j in cell k . Hence, $(j', k') \in q$ implies that UE k' in cell j' uses the same pilot as UE k in cell j .

ii. EW-MMSE Channel Estimator may be expressed in equation (8) as obtained in [15] and [17]:

$$\left[\hat{h}_{jk}^j \right]_m = \frac{\sqrt{p_{jk}} [R_{jk}^j]_{mm}}{\sum_{(j',k') \in q} p_{j'k'} \tau_p [R_{j'k'}^j]_{mm} + \sigma^2} y_{jk}^j \quad (8)$$

Where \hat{h}_{jk}^j is the EW-MMSE estimate of h_{jk}^j , [15-17].

iii. LS Channel Estimator may be expressed in equation (9) as obtained in [15] and [17]:

$$\hat{h}_{jk}^j = \frac{1}{\sqrt{p_{jk} \tau_p}} y_{jk}^j \quad (9)$$

Where \hat{h}_{jk}^j is the *LS estimate* of h_{jk}^j , the channel estimation quality is measured by the mean square error (MSE), $MSE = \left\| \hat{h}_{jk}^j - h_{jk}^j \right\|^2$ [15-16].

The matrices in transmit precoding may be defined by using the transmit powers P_j of all UEs in j th cell from BS j given in equation (10a)

$$P_j = \text{diag} (P_{j1}, P_{j2}, P_{j3} \dots P_{jk}) \in \mathbb{C}^{K \times K} \quad (10a)$$

Subscripts of estimated channel matrix \hat{H}_{jl} in Eqn. (10b) denote the channel connection between BS j and all the UEs in cell l with the MIMO DL channel.

$$\hat{H}_{jl} = \hat{h}_{lk}^j \quad (10b)$$

B. Downlink MMSE precoder

- i. Single-cell minimum mean squared error (S-MMSE): S-MMSE may be expressed in equation (11a) as obtained in [15].

$$F_j^{S-MMSE} = \left(\hat{H}_{jj} P_j (\hat{H}_{jj})^H + \sum_{i=1}^{K_j} p_{ji} C_{ji}^j + \sum_{\substack{l=1 \\ l \neq j}}^L \sum_{i=1}^{K_l} p_{li} R_{li}^j + \sigma^2 I_M \right)^{-1} \hat{H}_{jj} P_j \quad (11a)$$

- ii. Multi-cell minimum mean squared error (M-MMSE): M-MMSE may be expressed in equation (11b) as obtained in [15].

$$F_j^{M-MMSE} = \left(\sum_{l=1}^L \hat{H}_{jl} P_l (\hat{H}_{jl})^H + \sum_{l=1}^L \sum_{i=1}^{K_l} p_{li} C_{li}^j + \sigma^2 I_M \right)^{-1} \hat{H}_{jj} P_j \quad (11b)$$

P_l is transmitting powers of all UEs from BS j in cell l .

C. Power Precoding Normalization Techniques

The transmitted signal s_j in equation (1) may be expressed in [15] and [17] as:

$$s_j = \sum_{i=1}^{k_j} w_{ji} d_{ji} \quad (12a)$$

The transmitted signal s_j from j th BS antennas M in a cell consist of multiple information data signals d_{ji} that are transmitted. The transmitted signals make use of different precoding vectors w_{ji} from j th BS (e.g., different spatial directivity). If there are K UEs, a unit power DL data vector $d_{ji} = [d_{j1}, \dots, d_{jk}]$ from j th BS would be required for K different UEs in each cell. The transmitted signal s_j may be obtained by multiplying the precoding vector w_{ji} and the information DL data vectors d_{ji} . The precoding vector w_{ji} determines the direction of the spatial directivity of the DL data signals d_{ji} , while the squared norm $\|w_{ji}\|^2$ determines the associated transmit power.

$$W = [w_{j1}, \dots, w_{jK}] \quad (12b)$$

Where the precoding matrix $W \in \mathbb{C}^{M \times K}$ is defined as the $M \times K$ -dimensional precoding matrix and precoding vectors $w_{ji} \in \mathbb{C}^{M \times 1}$ are defined as the M -dimensional precoding vectors assigned to k th different UEs. Massive MIMO usually means that $\frac{M}{K} > 1$ and $M \gg K$. When the precoding vectors are selected, we need to ensure that too much transmit power is not used. Let the maximum downlink transmit power be P , P ($P_j = [P_{j1}, P_{j2}, P_{j3} \dots P_{jK}]^T$), the data vectors $d_{ji} = N_C(0, P)$ be modeled as a circularly symmetric complex Gaussian distribution having circular symmetry and N_C with zero mean. The $[P_{j1}, P_{j2}, P_{j3} \dots P_{jK}]$ are allocated from the j th BS to UEs in each cell and the squared Frobenius norm of W should equal the maximum transmit power [1-6] as expressed in equation (12c)

$$\|W\|_F^2 = P \quad (12c)$$

There are two types of power precoding normalization techniques viz: vector normalization (VN) and matrix normalization (MN) [1-6]. The major idea is to begin from an arbitrarily selected precoding matrix $F = [f_{j1}, \dots, f_{jK}]$ and then it is adapted into satisfying the power constraint.

1) Vector normalization (VN) technique: In this technique, we first normalize each column in matrix F to have a unit norm and all the entries are scaled with the same square root ratio of maximum transmit power P to number of UEs K . This satisfies equation (12c). We express the vector normalization technique as

$$W = \sqrt{\frac{P}{K}} \begin{bmatrix} \frac{f_1}{\|f_1\|} & \dots & \frac{f_K}{\|f_K\|} \end{bmatrix} \quad (13a)$$

One key merit is that the computation of the precoding vectors at BS j needs only MK complex multiplications, which are required to compute $\|f_k\|$ in equation (13a) for every UE [16].

2) Matrix normalization (MN) technique: In this technique, we select any precoding matrix F and all the entries are scaled with the square root of maximum transmit power P which is used to satisfy (12c). We express matrix normalization technique as

$$W = \frac{\sqrt{P}}{\|F\|_F} F \quad (13b)$$

The computation of the precoding matrix at BS j requires MK complex multiplications, which are needed to compute $\|F\|_F$ in equation (13b) for all UEs at once [3].

III. Downlink SINR, Downlink Spectral Efficiency (DL SE), and Network throughput

The expression for the effective downlink SINR as given in [15-17] is expressed in equation (14).

$$SINR_{jk}^{DL} = \frac{p_{jk} |\mathbb{E}\{w_{jk}^H h_{jk}^j\}|^2}{\sum_{l=1}^L \sum_{i=1}^K p_{li} |\mathbb{E}\{w_{li}^H h_{jk}^l\}|^2 - p_{jk} |\mathbb{E}\{w_{jk}^H h_{jk}^j\}|^2 + \sigma^2} \quad (14)$$

The expectation $\mathbb{E}\{\}$ is determined with reference to channel realizations. Therefore, a downlink SE maximizes the SINR in Eqn. (14) for a given channel estimate. The downlink SE is expressed in equation (15) as given in [15-17]:

$$SE_{jk}^{DL} = \frac{\tau_c - \tau_p}{\tau_c} \log_2(1 + SINR_{jk}^{DL}) \quad (15)$$

The term $\frac{\tau_c - \tau_p}{\tau_c}$ is the prelog factor that represents the portion of samples per coherence interval that are used for downlink data transmission. The network throughput (bits/s) is obtained by the multiplication of operational bandwidth (Hz) and SE (bits/s/Hz).

$$Network\ throughput \left(\frac{bit}{s} \right) = Bandwidth\ (Hz) \times SE_{jk}^{DL} \left(\frac{bit}{s/Hz} \right) \quad (16)$$

IV. Simulation, Results and Discussion

A square pattern network layout is used in [15-17]. The 16-cell setup is utilized and each cell has an area of 1 km². Inter-cell and intra-cell interference received by all the base stations are the same in all directions. The value of the large-scale fading coefficient, path loss factor and standard deviation, operating bandwidth is as given in [15]. A 100mW downlink transmit power was allocated to each UE in a particular cell and the number of UEs per cell given as 10 [15]. The UEs were equally distributed in each cell. A channel characterized by uniform local scattering (ULA) and correlated Rayleigh fading with a value of angular standard deviation (ASD) of 10° (degree) was used. The downlink throughput, SE, and SINR/SNR were computed and simulated to obtain numerical results. The simulation parameters are tabulated in table 1.

Table 1: Simulation Parameters

Parameter	Value
Network layout	Square pattern (wrap-around)
Cell area	1km × 1km
Number of BS antennas	100
Number of Cells	16

Number of UEs (or users) in each cell	10
Communication Bandwidth	$B = 20$ MHz
DL transmit power	100mW (-10dB)
Noise Figure	7dB
Noise Variance	$-174 + 10 \log_{10} B + \text{Noise Figure}$
Pathloss exponent	3.76
Shadow fading (standard deviation)	10
Distance between UE k in cell l and BS j	d_{lk}^j
Average channel gain using the large-scale fading model	$-35.3 - 37.6 \log_{10} d_{lk}^j$
Pilot reuse factor f	1, 2, 4 or 16
Total coherence block length (τ_c)	200
Number of pilot sequences (τ_p)	fK
Channel Model	Uniform local scattering model and correlated Rayleigh fading channel
Angular standard deviation	10° (degree)
Number of channel realizations	10
Number of random setup	1

-Impact on Network throughput

Network throughput is one of the vital metric to evaluate network performance in mMIMO networks. This metric is expressed in equation (16) and measures the quality of service (QoS) of the network. In order to examine the impact of throughput on the performance of the compared precoders, the three different estimators discussed in section (II)A were introduced into the simulation as shown in figures 1 –3.

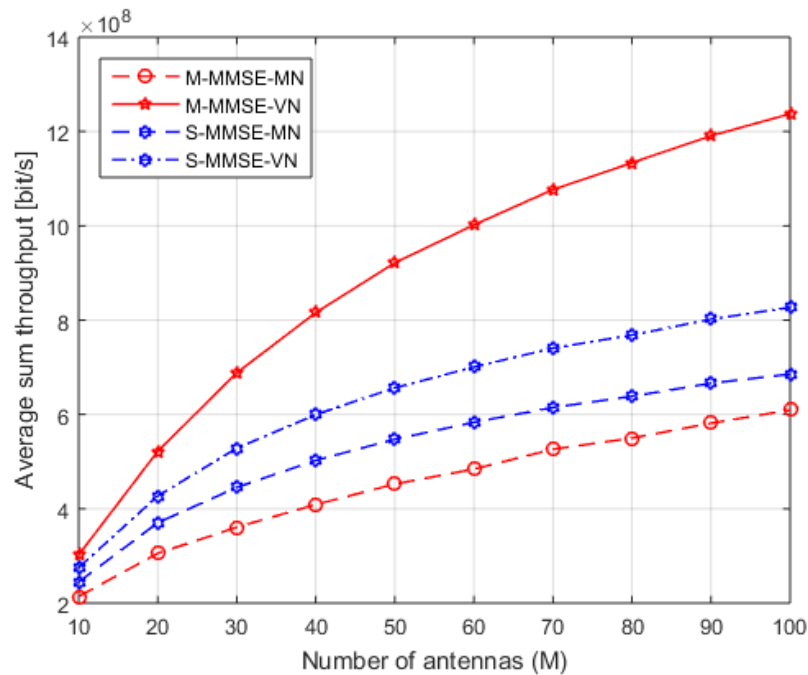


Figure 1: Throughput vs. Number of antennas (M) for $K = 10$ UEs and $f = 4$ with the MMSE estimator.

Figure 1 depicts the average DL sum throughput plotted against the number of antennas with MMSE channel estimates using power normalization when the pilot reuse factor is 4 ($f = 4$). M-MMSE with vector normalization (VN) has the highest average sum throughput for any number of antennas and passes from 3.10×10^8 bit/s to 12.37×10^8 bit/s as the number of antenna increases. M-MMSE with matrix normalization (MN) has the lowest average sum throughput for any number of antennas. S-MMSE with vector normalization (VN) performs better than S-MMSE with matrix normalization (MN). The downlink throughput comparison of the two basic linear precoding techniques with MMSE channel estimation and pilot reuse factors of 1, 2, 4, and 16 under power normalization are presented in table 2. The values of the precoding techniques when $f = 4$ are in bold face in table 2

Table 2: Downlink throughput (bit/s) for MMSE Channel Estimator with $M=100$, $K = 10$, and different pilot reuse factor ($f = 1, 2, 4$, and 16).

MMSE Channel Estimates for $M = 100$				
Precoding technique	Pilot reuse factor (Throughput)			
	$f = 1$	$f = 2$	$f = 4$	$f = 16$
M-MMSE-MN	7.634E+08	7.018E+08	6.094E+08	1.623E+08
M-MMSE-VN	1.397E+09	1.357E+09	1.237E+09	3.337E+08
S-MMSE-MN	8.296E+08	7.767E+08	6.854E+08	1.634E+08
S-MMSE-VN	1.036E+09	9.454E+08	8.27E+08	2.271E+08

We compare the percentage performance of precoding techniques using figure 1 and table 2 with respect to the method applied in [15].

$$S\text{-MMSE-VN} = \frac{8.27E+08}{1.237E+09} \times 100 = 66.86\% \text{ of the sum throughput generated by M-MMSE-VN.}$$

$$S\text{-MMSE-MN} = \frac{6.854E+08}{1.237E+09} \times 100 = 55.40\% \text{ of the sum throughput generated by M-MMSE-VN.}$$

$$M\text{-MMSE-MN} = \frac{6.094E+08}{1.237E+09} \times 100 = 49.26\% \text{ of the sum throughput generated by M-MMSE-VN.}$$

The M-MMSE-MN technique gives 50.74% lower throughput than M-MMSE-VN, but 6.14% lower throughput than S-MMSE-MN and 17.6% lower throughput than S-MMSE-VN.

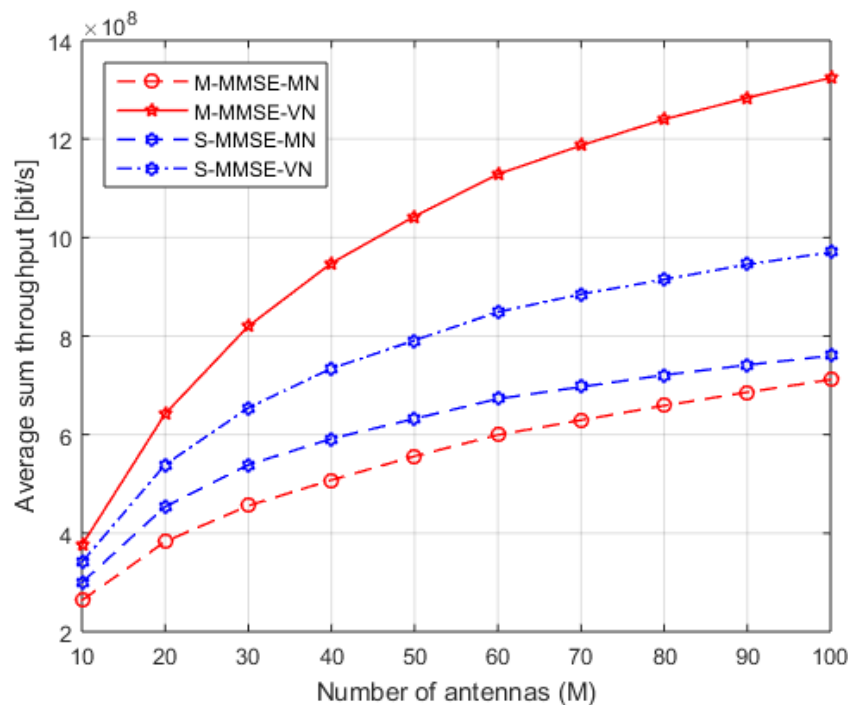


Figure 2: Throughput vs. Number of antennas (M) for $K = 10$ UEs and $f = 4$ with the EW-MMSE estimation.

Figure 2 depicts the average DL sum throughput plotted against the number of antennas with the EW-MMSE Channel Estimates using power normalization when the pilot reuse factor is 4 ($f = 4$). M-MMSE with vector normalization (VN) has the highest average sum throughput for any number of antennas and passes from 3.93×10^8 bit/s to 13.24×10^8 bit/s as M increases while M-MMSE with matrix normalization (MN) has the lowest average sum throughput for any number of antennas and passes from 2.87×10^8 bit/s to 7.12×10^8 bit/s as the number of antenna increases. S-MMSE with vector normalization (VN) performs better than S-MMSE with matrix normalization (MN). MN produces the same precoding weight among UEs by normalizing over all UEs while VN conducts precoding for each UE individually, which results in different throughput among UEs. The downlink throughput comparison of the two basic linear precoding techniques with EW-MMSE channel estimation and pilot reuse factor of 1, 2, 4 and 16 under power normalization are presented in table 3 with the values of the precoding techniques when $f = 4$ in bold face.

Table 3: Downlink throughput (bit/s) for EW-MMSE Channel Estimator with $M=100$, $K = 10$, and different pilot reuse factor ($f = 1, 2, 4, \text{ and } 16$).

EW-MMSE Channel Estimates for M = 100				
Precoding technique	Pilot reuse factor (Throughput)			
	$f = 1$	$f = 2$	$f = 4$	$f = 16$
M-MMSE-MN	7.517E+08	7.963E+08	7.115E+08	1.604E+08
M-MMSE-VN	1.167E+09	1.379E+09	1.324E+09	3.407E+08
S-MMSE-MN	8.395E+08	8.636E+08	7.6E+08	1.651E+08
S-MMSE-VN	1.118E+09	1.128E+09	9.699E+08	2.36E+08

We compare the percentage performance of precoding techniques using figure 2 and table 3 in respect to the method applied in [15].

$$S\text{-MMSE-VN} = \frac{9.699E+08}{1.324E+09} \times 100 = 73.26\% \text{ of the sum throughput generated by M-MMSE-VN.}$$

$$S\text{-MMSE-MN} = \frac{7.6E+08}{1.324E+09} \times 100 = 57.40\% \text{ of the sum throughput generated by M-MMSE-VN.}$$

$$M\text{-MMSE-MN} = \frac{7.115E+08}{1.324E+09} \times 100 = 53.74\% \text{ of the sum throughput generated by M-MMSE-VN.}$$

The S-MMSE-VN technique gives 26.74% lower throughput than M-MMSE-VN, but 15.86% higher throughput than S-MMSE-MN and 19.52% higher throughput than M-MMSE-MN. For example, the sum throughput of M-MMSE precoding with VN (when $M = 20$) achieves the same performance as M-MMSE precoding with MN (when $M = 70$). Figures 1 and 2 depict that the number of antennas M required to achieve a target sum throughput in MMSE and EW-MMSE channel estimates using M-MMSE precoding technique with matrix normalization (MN) is higher than the one required by vector normalization (VN) by a factor of $3\frac{1}{2}$.

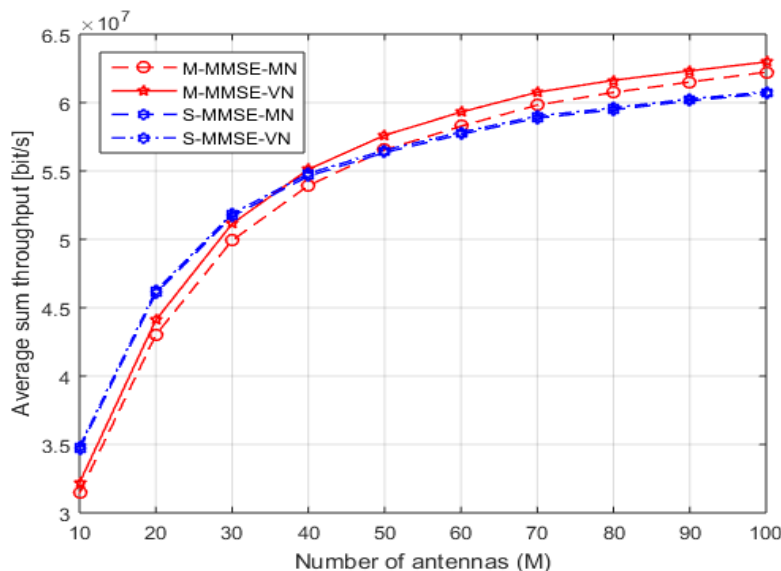


Figure 3: Throughput vs. Number of antennas (M) for $K = 10$ UEs and $f = 4$ with LS estimation.

Figure 3 presents the average DL sum throughput plotted against the number of antennas with LS channel estimates using power normalization when the pilot reuse factor is 4 ($f = 4$). M-MMSE with vector normalization (VN) has the highest average sum throughput from the point when the number of antennas is greater than or equal to 40 ($M \geq 40$) while M-MMSE with matrix normalization (MN) has the lowest average sum throughput from the point when the number of antennas is less than or equal to 40 ($M \leq 40$). S-MMSE with vector normalization (VN) and matrix normalization (MN) has the same sum throughput value, which ranges from 3.51×10^7 bit/s to 6.07×10^7 bit/s as the number of antenna increases. The downlink throughput comparison of the two basic linear precoding techniques with LS channel estimation and pilot reuse factor of 1, 2, 4 and 16 under power normalization are presented in table 4 with the values of the precoding techniques when $f = 4$ in bold face.

Table 4: Downlink throughput (bit/s) for LS Channel Estimator with $M=100$, $K =10$, and different pilot reuse factor ($f =1, 2, 4$, and 16).

LS Channel Estimates for M = 100				
Precoding technique	Pilot reuse factor (Throughput)			
	$f = 1$	$f = 2$	$f = 4$	$f = 16$
M-MMSE-MN	1.759E+07	3.384E+07	6.223E+07	1.528E+08
M-MMSE-VN	1.762E+07	3.4E+07	6.297E+07	3.001E+08
S-MMSE-MN	1.767E+07	3.32E+07	6.065E+07	1.471E+08
S-MMSE-VN	1.768E+07	3.32E+07	6.079E+07	2.106E+08

We compare the percentage performance of precoding techniques using figure 3 and table 3 by applying the methods used in [15].

$$S\text{-MMSE-VN} = \frac{6.079E+07}{6.297E+07} \times 100 = 96.53\% \text{ of the sum throughput generated by M-MMSE-VN.}$$

$$S\text{-MMSE-MN} = \frac{6.065E+07}{6.297E+07} \times 100 = 96.32\% \text{ of the sum throughput generated by M-MMSE-VN.}$$

M-MMSE-MN = $\frac{6.223E+07}{6.297E+07} \times 100 = 98.82\%$ of the sum throughput generated by M-MMSE-VN. The M-MMSE-MN technique gives 1.18% lower throughput than M-MMSE-VN, but 2.5% higher throughput than S-MMSE-MN and 2.26% higher throughput than S-MMSE-VN.

-Impact on SE

This metric is expressed in equation (15), we simulated the SE by increasing the number of UEs in the cells, to evaluate the performance of the network. Figures 4 - 6 compares the effect of the different estimators on the SE metric.

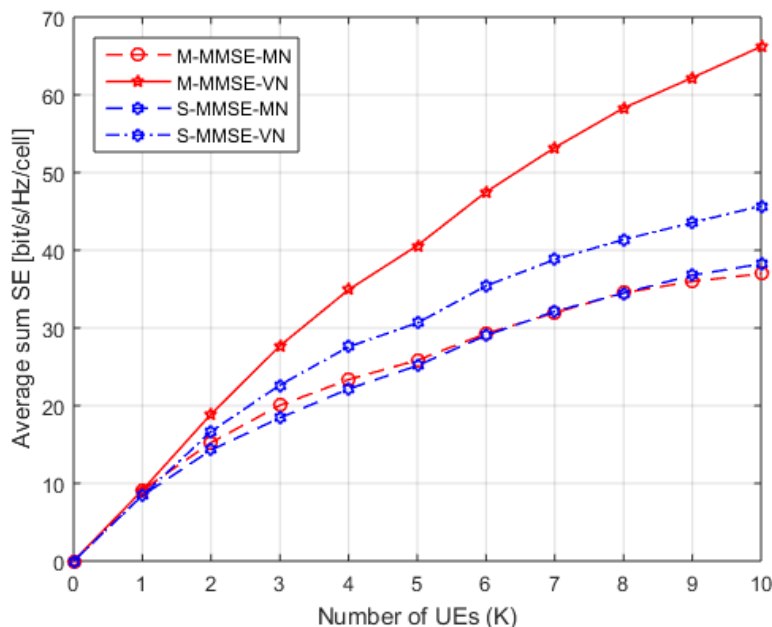


Figure 4: Downlink SE vs. Number of UEs (K) for M = 100 antennas and $f = 4$ with MMSE estimation.

Figure 4 shows the average DL sum SE as a function of the number of UEs with MMSE channel estimates using power normalization when the pilot reuse factor is 4 ($f = 4$). M-MMSE and S-MMSE with vector normalization (VN) have higher average sum SE than S-MMSE and M-MMSE with matrix normalization (MN) when the number of UEs is more than 1 ($UE > 1$). This is because of the expectation $\mathbb{E}\left\{\sqrt{\frac{P}{K}}\right\}$ which implies that the same transmit power is assigned to UEs in VN.

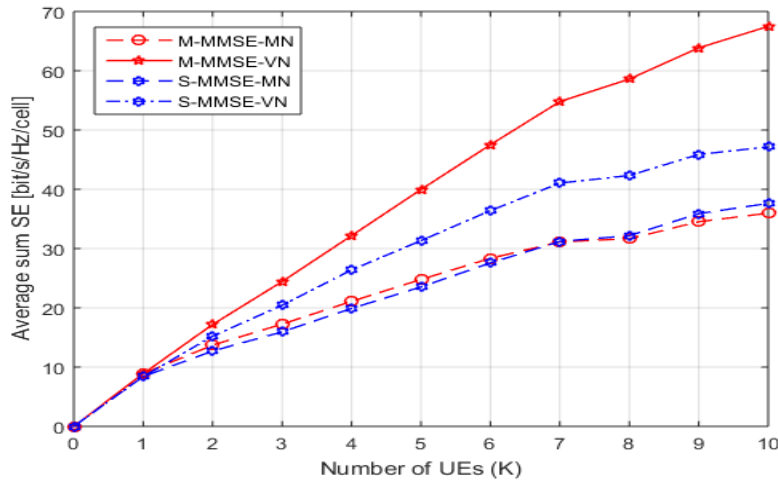


Figure 5: Downlink SE vs. Number of UEs (K) for M = 100 antennas and f = 4 with EW-MMSE estimation.

Figure 5 shows the average DL sum SE as a function of the number of UEs with EW-MMSE channel estimates using power normalization when the pilot reuse factor is 4 ($f = 4$). M-MMSE and S-MMSE with vector normalization (VN) have higher average sum SE than S-MMSE and M-MMSE with matrix normalization (MN) when the number of UEs is more than 1 ($UE > 1$). For $UE > 1$, the expectation becomes $\mathbb{E}\left\{\frac{\sqrt{P}}{\sqrt{|F|_F}}\right\}$, hence different transmit powers are assigned to UEs in MN. For example, in the above figures, the sum SE of M-MMSE precoding with VN (when $K = 3$) achieves the same performance as M-MMSE precoding with MN (when $K = 5$). Figures 4 and 5 show that the number of UEs K required to achieve a target sum SE in MMSE and EW-MMSE channel estimates using M-MMSE precoding technique with vector normalization (VN) is smaller than the one required by matrix normalization (MN) by a factor of $1\frac{1}{2}$ ($5/3$).

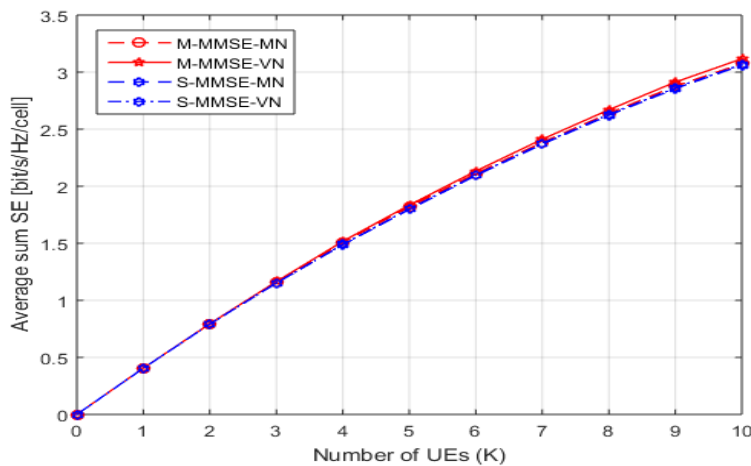


Figure 6: Downlink SE vs. Number of UEs (K) for M = 100 antennas and f = 4 with LS estimation.

Figure 6 presents the average DL sum SE as a function of the number of UEs with LS channel estimates using power normalization when the pilot reuse factor is 4 ($f = 4$). M-MMSE with vector normalization (VN) performs better than S-MMSE with vector/matrix normalization and M-MMSE with matrix normalization (MN). It is observed from figures 4, 5, and 6 that as the number of UEs (K) per cell rises, the average sum SE rises. In general, it is observed that M-MMSE with vector normalization (VN) precoding technique has the highest SE with an increase in UEs when compared to the S-MMSE with vector/matrix normalization and M-MMSE with matrix normalization (MN). VN performs precoding for each UEs separately, which generates different SE among UEs. In contrast, MN produces the same precoding weight among UEs by normalizing over all UEs.

-Impact on SNR

The signal-to-noise ratio (SNR) as a performance metric in the mMIMO networks generally depends on three parameters namely the transmit power, channel gain, and noise power [16]. The SNR in this case is used only to evaluate the transmit power of the BS where the other parameters are normalized to unity. Figures 7 - 9 compares different SNR values resulting from the three different channel estimates.

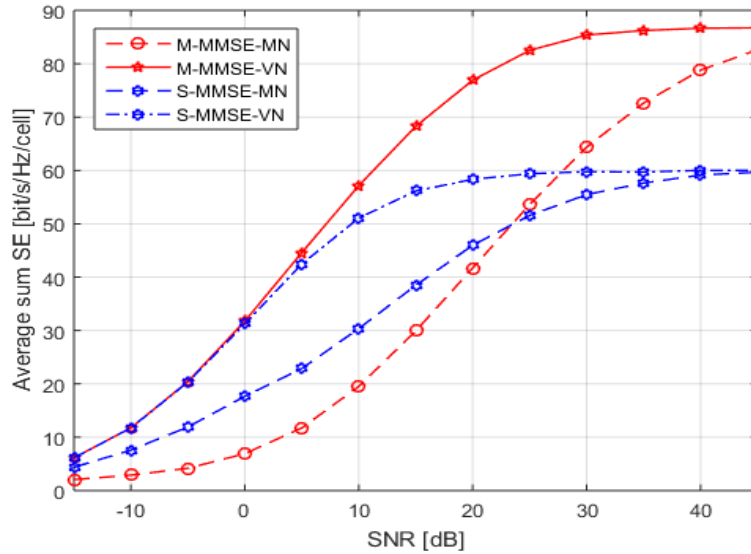


Figure 7: Downlink SE vs. Signal to Noise [dB] for $M = 100$ antennas and $f = 4$ with MMSE estimation.

Figure 7 shows the average DL sum SE as a function of SNR with MMSE Channel Estimates using power normalization when the pilot reuse factor is 4 ($f = 4$). M-MMSE with vector normalization (VN) has a superior performance than S-MMSE with vector/matrix normalization and M-MMSE with matrix normalization (MN). There is a finite increase in the SE of M-MMSE with vector and matrix normalization at SNR from -15 dB to 40dB. The S-MMSE-VN has a better SE than S-MMSE-MN at SNR of -15dB to 20 dB. At $SNR \geq 40$ dB, the slope of the graph becomes relatively steadier up to the SE value of 60bit/s/Hz.

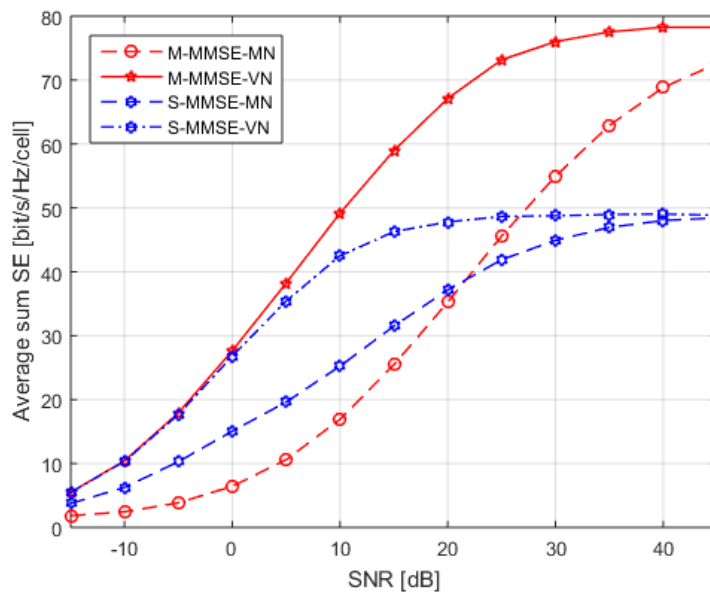


Figure 8: Downlink SE vs. Signal to Noise [dB] for $M = 100$ antennas and $f = 4$ with EW-MMSE estimation.

Figure 8 gives the average DL sum SE as a function of SNR with EW-MMSE channel estimates using power normalization when the pilot reuse factor is 4 ($f = 4$). M-MMSE with vector normalization (VN) has a better performance than S-MMSE with vector/matrix normalization and M-MMSE with matrix normalization (MN). There is a finite increase in SE of M-MMSE with vector and matrix normalization at SNR from -15 dB to 40dB. The S-MMSE with vector normalization has a better performance

than S-MMSE with matrix normalization (MN) at low SNR from -15dB to 20 dB and after SNR ≥ 20 dB the slope becomes relatively steadier at SE value of 48bit/s/Hz.

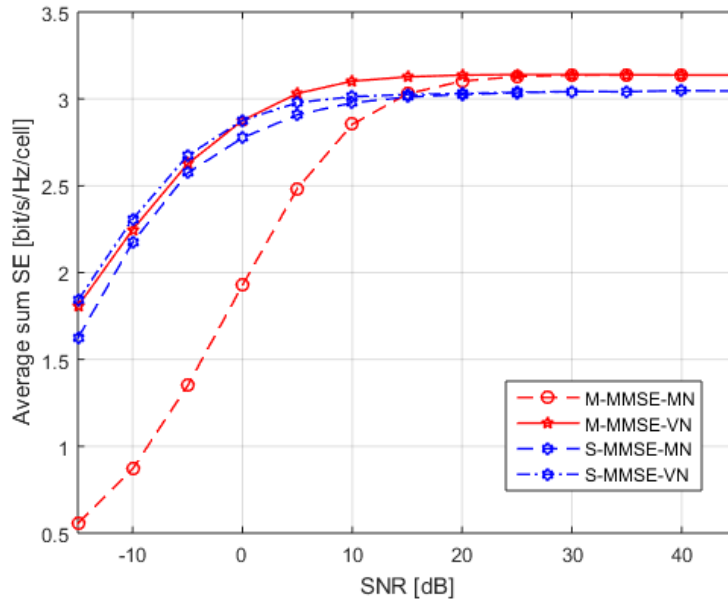


Figure 9: Downlink SE vs. Signal to Noise [dB] for M = 100 antennas and f = 4 with LS estimation.

Figure 9 shows the average DL sum SE as a function of SNR with LS channel estimates using power normalization when the pilot reuse factor is 4 ($f = 4$). There is a finite increase in SE of M-MMSE with vector/ matrix normalization and S-MMSE with vector/ matrix normalization at low SNR from -15 dB to 10dB. M-MMSE with vector and matrix normalization has a better performance than S-MMSE with vector and matrix normalization at high SNR from 20dB to 45dB. The complex analysis associated with M-MMSE is higher than that of S-MMSE because of inter-cell interference suppression. In general, figures 7, 8, and 9 show that the M-MMSE-VN precoding technique has better performances when compared to the M-MMSE-MN and S-MMSE-VN/S-MMSE-MN. The M-MMSE-VN precoding technique performs best at both high and low SNR. From figures 7, 8, and 9 it can be inferred that an increase in the transmit power can boost the SE of massive MIMO networks. This is because as transmit power of the BS antennas increases, the sum SE increases.

-Impact on SINR

SINR is a performance metric used to measure the desired signal to interference plus noise ratio. This metric is expressed in equation (16). The SINR was simulated by increasing the number of antennas in the mMIMO network. The results for the three different estimators are presented in figures 10 – 12.

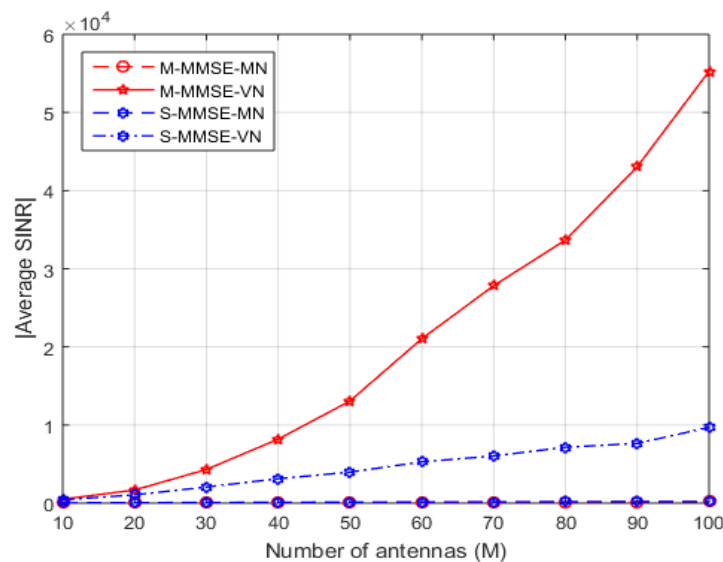


Figure 10: Average SINR vs. Number of antennas (M) for K = 10 UEs and f = 4 with MMSE estimation.

Figure 10 presents the average SINR as a function of the number of antennas with MMSE channel estimates using power normalization when the pilot reuse factor is 4 ($f = 4$). M-MMSE-VN has the highest SINR for any number of antennas while M-MMSE-MN and S-MMSE-MN performed poorly because $\mathbb{E}\left\{\frac{F}{\|F\|_F}\right\}$ is unknown and produces the same precoding weight among UEs by normalizing over all UEs.

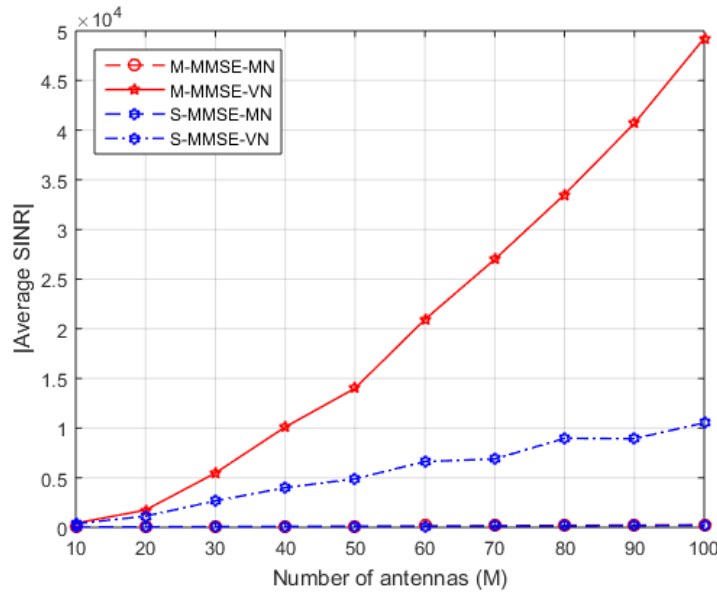


Figure 11: Average SINR vs. Number of antennas (M) for K = 10 UEs and f = 4 with EW-MMSE estimation.

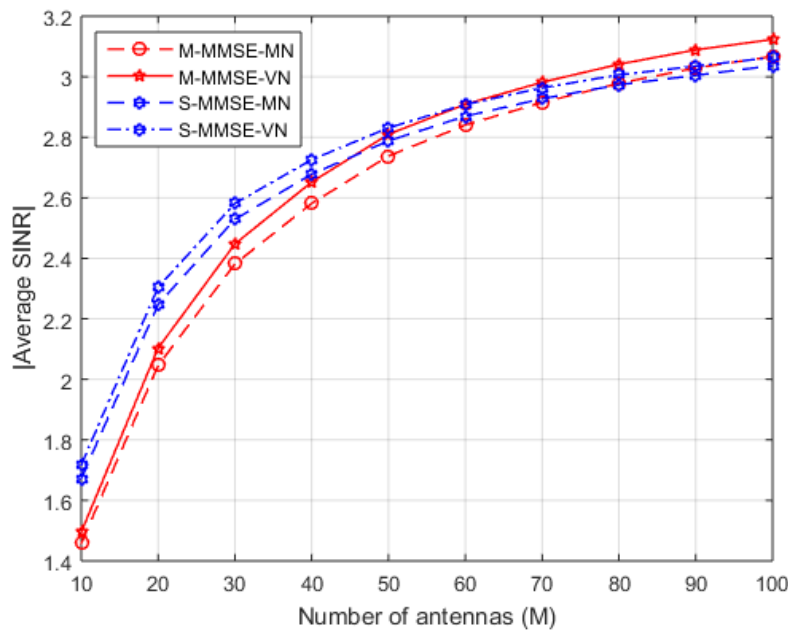


Figure 12: Average SINR vs. Number of antennas (M) for K = 10 UEs and f = 4 with LS estimation.

Figure 11 presents the average SINR plotted against the number of antennas with the MMSE channel estimates using power normalization when the pilot reuse factor is 4 ($f = 4$). M-MMSE with vector normalization (VN) has the highest SINR for any number of antennas while M-MMSE and S-MMSE with matrix normalization (MN) performed poorly. Figure 12 shows the average SINR plotted against the number of antennas with LS channel estimates using power normalization when the pilot reuse factor is 4 ($f = 4$). S-MMSE with vector/matrix normalization performs better than M-MMSE with vector/matrix normalization when the number of antennas is less than 50 ($M < 50$). In Figure 10, 11, and 12, the signal to interference plus noise ratio (SINR) increases linearly with the number of base station antennas and does not saturate as the number of base station antennas tend to infinity.

V. Conclusion

Massive MIMO technology is one of the key enabling technologies for new and future generation wireless communication networks. It can increase the throughput and SE. Massive MIMO has been used in this work to show the power normalization effects on linear precoding techniques at the BS and on channel estimation via a downlink. The above figures show throughput, SE, and SNR (or SINR) performance metrics with two basic precoding techniques such as M-MMSE and S-MMSE using vector normalization (VN) and matrix normalization (MN) respectively. MMSE and EW-MMSE estimators produced the highest average sum SEs while LS estimator produced the lowest average sum SEs. There is a significantly large percentage loss of average sum SE if the LS estimator is used. LS estimator performs poorly when compared to EW-MMSE and MMSE estimators. The SE, throughput, and SINR (or SNR) are not much improved even if the pilot reuse factor f is increased. Numerical results showed that M-MMSE-VN and S-MMSE-VN are effective at achieving higher SE, throughput, and SNR (or SINR) than M-MMSE-MN and S-MMSE-MN. However, transmit power is fairly assigned to UEs in MN than in VN for practical scenarios. In future work, we will consider the issue of using power normalization on non-linear precoding techniques with optimization algorithms to solve different power allocation issues.

VI. References

1. Björnson, E., Sanguinetti, L., Wymeersch H., Hoydis, J., and Marzetta, T. L., (2019) Massive MIMO is a reality—what is next? Five promising research directions for antenna arrays, *Digital Signal Processing*, Elsevier, 94(1), 3–20.
2. Albreem, M. A., Alhabbash, A., Abu-Hudrouss, A. M., and Ikki, S., (2021) Overview of Precoding Techniques for Massive MIMO, *IEEE Access*.
3. Albreem, M. A., Juntti, M., and Shahabuddin, S., (2019) Massive MIMO detection techniques: A survey, *IEEE Commun. Surveys Tuts.*, 21(4), 3109–3132.
4. Segneri, A., Baldominos, A., Goussetis, G., Mengali, A. and Fonseca, N.J.G., (2022) Closed-Form Power Normalization Methods for a Satellite MIMO System, *Sensors*, 22(7).
5. Sadeghi, M., Sanguinetti, L., Couillet, R., and Yuen, C., (2017) Large system analysis of power normalization techniques in Massive MIMO, *IEEE Trans. Veh. Technol.*, 66(10), 9005–9017.
6. Thurpati, S., Mudavath, M., and Muthu Chidambar Nathan, P., (2021) Performance Analysis of Linear Precoding in Downlink Based on Polynomial Expansion on Massive MIMO Systems, *Journal of Physics: Conference Series*.
7. Mohammad, M. A. B., Osman, A. A. and Elhag, N. A. A., (2015) Performance Comparison of MRT and ZF for Single Cell Downlink Massive MIMO System, *IEEE International Conference on Computing, Control, Networking, Electronics and Embedded Systems Engineering*.
8. Ali, M. A. Ibrahim, and Murtada, M. Abdelwahab, (2017) Sum Rate Analysis of Massive Multiple Input Multiple Output System for Linear Precoding using Normalization Methods, *IEEE International Conference on Communication, Control, Computing and Electronics Engineering (ICCCCEE)*, Khartoum, Sudan.
9. Lee, C., Chae, C-B., Kim, T., Choi, S., and Lee, J., (2012) Network Massive MIMO for Cell-Boundary Users: From a Precoding Normalization Perspective, *IEEE International Workshop on Cloud Base-Station and Large-Scale Cooperative Communications*.
10. Lim, Y-G., Chae, C-B., and Caire, G., (2015) Performance analysis of massive MIMO for cell-boundary users, *IEEE Trans. Wireless Commun.*, 14(12), 6827–6842.
11. Sadeghi, M., Sanguinetti, L., Couillet, R., and Yuen, C., (2016) Power Normalization in Massive MIMO Systems: How to Scale Down the Number of Antennas, *IEEE International Conference on Communications*, Kuala Lumpur, Malaysia.
12. Mizutani, R., Shimbo, Y., Saganuma, H., and Maehara, F., (2018) Impact of Power Normalization on System-Level Performance in MU-MIMO with User Scheduling, *2018 International Symposium on Antennas and Propagation (ISAP 2018)*.
13. Li, X., Bjornson, E., Larsson, E. G., Zhou, S., and Wang, J. (2015) A multicell MMSE precoder for massive MIMO systems and new large system analysis, in *IEEE Int. Conf. Global Commun. (GLOBECOM)*, San Diego, CA, 1–6.
14. Li, X., Bjornson, E., Larsson, E. G., Zhou, S., and Wang, J. (2017) Massive MIMO with multi-cell MMSE processing: exploiting all pilots for interference suppression, *EURASIP Journal on Wireless Communications and Networking*.
15. Bjornson, E., Hoydis, J., and Sanguinetti, L., (2017) Massive MIMO Networks: Spectral, Energy, and Hardware Efficiency, *Foundations and Trends in Signal Processing*, 11(3-4), 154–655.
16. Sanguinetti, L., Bjornson, E., and Hoydis, J., (2019) Towards Massive MIMO 2.0: Understanding spatial correlation, interference suppression, and pilot contamination, *IEEE Transactions on Communications*, 0090-6778.
17. Özdogan, Ö., Bjornson, E., and Larsson, E. G., (2019) Massive MIMO with Spatially Correlated Rician Fading Channels, *IEEE Transactions on Communications*.
18. Singh, J., and Kedia, D., (2020) Spectral Efficient Precoding Design for Multi-cell Large MU-MIMO System, *IETE Journal of Research*, 1–17.
19. Waleed, A. Ali, Wagdy, R. Anis, and Hamed, A. Elshenawy, (2020) Spectral efficiency enhancement in Massive MIMO system under pilot contamination, *Int. J Commun Syst*.
20. Eze, G.C., (2022) Multi-Cell Linear Precoders for massive MIMO with Matrix Normalization, *International Journal of Scientific & Engineering Research*, 13(11), 243–250.